Geophys. J. Int. (1991) **107**, 77–82

Spherical harmonic representation of the gravitational potential of discrete spherical mass elements

Stephen T. Sutton,* Henry N. Pollack and Michael J. Jackson†
Department of Geological Sciences, The University of Michigan, Ann Arbor, MI 48109, USA

Accepted 1991 April 29. Received 1991 April 29; in original form 1990 August 28

SUMMARY

We present expressions in a spherical harmonic framework for the gravitational potential of discrete point, surface, and volume mass elements located at any depth within a sphere. Through analysis of the spherical harmonic spectrum, insight is gained into the properties of the potentials arising from a variety of mass distributions. A point mass at the surface of a sphere displays the richest harmonic spectrum in all degrees; spectra become increasingly reddened as the source mass is distributed through larger elements of area or volume, or is located at greater depths below the surface of the reference sphere. The spectra of dipolar distributions, useful in representing compensated masses, are depressed, especially in the low harmonic degrees, relative to the spectra of monopole elements.

Key words: geoid, gravity, potential.

1 INTRODUCTION

In this paper we develop the spherical harmonic framework for expressing the gravitational potential of several discrete mass elements located arbitrarily within a sphere. These include a point mass, a point dipole, a spherical cap and a spherical rectangle, as well as the radial extension of the 2-D elements through some volume. We also discuss aspects of the use of these elements in modelling the potential field of the earth. In an accompanying paper (Jackson, Pollack & Sutton, this issue, paper II) we carry out forward models of the Earth's potential spectrum, using these discrete anomalous mass elements.

Numerous workers have used point masses as elements in models of planetary density structure (Chase 1979; Chase & McNutt 1982; Crough & Jurdy 1980; Lowrey 1978; Reasenberg *et al.* 1981; Sjogren, Bills & Mottinger 1984). As an alternative or complement to point masses, workers have also commonly used distributed mass elements. The literature of applied geophysics contains a plethora of formulae within a Cartesian or 'flat earth' system for the gravitational potential or attraction of a great variety of distributed masses, many of which are summarized by Talwani (1973).

For planetary-scale models of gravitational fields, analogous expressions for the potential or attraction of distributed mass elements within a framework of spherical or ellipsoidal coordinates are both more useful and less readily available than the equivalent expressions in rectangular coordinates. Takin & Talwani (1966) and Bowin, Simon & Wollenhaupt (1975) modify the scheme of Talwani & Ewing (1960) for the attraction of an arbitrary solid in Cartesian coordinates to obtain corrections leading to an approximation of the attraction due to a similar body in a spherical system. Johnson & Litehiser (1972) develop a more direct method for computing the gravitational attraction of a 3-D body represented by a set of polygonal spherical laminae. They obtain the attraction via a mixture of analytic and numerical integration. Hellinger (1983) further refines this approach.

Purely analytic solutions for the potential of distributed bodies in a spherical harmonic framework are quite useful. Once computed, the coefficients of a spherical harmonic expansion allow relatively simple determination of the gravitational potential at any point outside the reference sphere. Direct computation of the spherical harmonic coefficients also facilitates spectral analysis of a disturbing potential. Pollack (1973) presents expressions in a spherical harmonic framework for the potential of a point mass, a spherical cap, and a spherical rectangle located at the surface of a planet, and discusses the spherical harmonic spectra associated with these mass elements. In a similar fashion, McAdoo (1981) develops the spherical harmonic expression for the potential due to a great circle ring source, and examines its spectral properties. In this paper we extend the 2-D elements of Pollack (1973) through the radial dimension to obtain their respective 3-D analogues, the spherical cone and the spherical block, and analytically

* Currently at Exxon Company International, Houston TX, USA.
† Currently at University of Minnesota, Minneapolis MN, USA.

derive the spherical harmonic coefficients for the external potential due to these distributed sources.

2 ANALYSIS

2.1 Introduction

The following symbols, mostly following those of Pollack (1973), will be used in the analytical development.

r	distance from coordinate origin to field point
ϕ	colatitude of field point
μ	$=\cos\phi$
θ	longitude of field point
r'	distance from coordinate origin to point mass, point dipole, infinitesimal mass element, or pole of spherical cap or truncated cone
ϕ'	colatitude of point mass, point dipole, infinitesimal mass element, or pole of spherical cap or truncated cone
μ'	$=\cos\phi'$
θ'	longitude of point mass, point dipole, infinitesimal mass element, or pole of spherical cap or truncated cone
a	radius of sphere in which discrete masses are located
α	generating angle of spherical cap or truncated cone
λ	$=\cos\alpha$
Ω	solid angle, with respect to the centre of a sphere of radius a, subtended by any mass element
σ	areal density of surface mass distributions
ρ	volumetric density of masses distributed through an element of volume
V	gravitational potential
M	total mass of an ensemble of mass elements
M_i	mass of the ith mass element in an ensemble of mass elements
${}_iM_r$	gravitational moment of a point dipole oriented radially
G	Newtonian gravitational constant
$\bar{P}_{nm}(\mu)$	fully normalized associated Legendre function of degree n and order m (absence of overbar indicates unnormalized function)
$\bar{R}_{nm}(\mu, \theta)$, $\bar{S}_{nm}(\mu, \theta)$	fully normalized surface spherical harmonic functions of degree n and order m
$\bar{J}_{nm}$, $\bar{K}_{nm}$	coefficients of fully normalized spherical harmonic expansion of gravitational potential
σ_n^2	variance of harmonic coefficients of degree n
Φ_n	$=(2n+1)^{1/2}\sigma_n$

The following definitions and relationships are used in the analysis (Heiskanen & Moritz 1967):

$$\bar{P}_{n0}(\mu)=\bar{P}_n(\mu)=(2n+1)^{1/2}P_{n0}(\mu), \tag{1a}$$

$$\bar{P}_{nm}(\mu)=[2(2n+1)(n-m)!/(n+m)!]^{1/2}P_{nm}(\mu), \tag{1b}$$

$$\begin{bmatrix}\bar{R}_{nm}(\mu,\theta)\\ \bar{S}_{nm}(\mu,\theta)\end{bmatrix}=\bar{P}_{nm}(\mu)\begin{bmatrix}\cos(m,\theta)\\ \sin(m,\theta)\end{bmatrix}. \tag{2}$$

The potential of a spherical body of radius a and total mass M containing an ensemble of discrete mass anomalies can be represented by

$$V=(GM/r)\Big\{1-\sum_{n=1}^{\infty}\sum_{m=0}^{n}(a/r)^n[\bar{J}_{nm}\bar{R}_{nm}(\mu,\theta)+\bar{K}_{nm}\bar{S}_{nm}(\mu,\theta)]\Big\}. \tag{3}$$

The potential coefficients J_{nm} and K_{nm} represent the integrated effects of the mass anomalies. These coefficients are given by the sum of the coefficients for each of the k elements comprising the ensemble:

$$\begin{bmatrix}\bar{J}_{nm}\\ \bar{K}_{nm}\end{bmatrix}=\sum_{i=1}^{k}\begin{bmatrix}{}_i\bar{J}_{nm}\\ {}_i\bar{K}_{nm}\end{bmatrix}. \tag{4}$$

Here the coefficients for an individual mass element are subscripted by the index i; the coefficients for the entire ensemble are not so indexed. Each coefficient ${}_iJ_{nm}$ or ${}_iK_{nm}$ is a function of the size, shape, mass, and location of the ith anomalous element. We may take

$$M=M_s+\sum_{i=1}^{k}M_i,$$

where M_i is the mass of the ith disturbing element. The sum may be zero or even negative. M_s is the central mass added to the sum of the disturbing masses in order to yield a total mass M. If M is the mass of the Earth, the disturbing masses M_i will generally be several orders of magnitude smaller.

Pollack (1973) presents expressions for the coefficients of the potential due to a point mass, a spherical cap, and a spherical rectangle at the surface of a sphere. Fig. 1 illustrates these elements. Those results for mass elements at the surface of the sphere can easily be generalized for a mass element at any radius r' within the sphere. The coefficients for the potential of a point mass, spherical cap and spherical rectangle of mass M_i at arbitrary depth are given by

$$\begin{bmatrix}{}_i\bar{J}_{nm}\\ {}_i\bar{K}_{nm}\end{bmatrix}=\frac{-1}{2n+1}\left(\frac{r_i'}{a}\right)^n\left(\frac{M_i}{M}\right)\begin{bmatrix}\bar{R}_{nm}(\mu_i',\theta_i')\\ \bar{S}_{nm}(\mu_i',\theta_i')\end{bmatrix}, \tag{5}$$

point

$$\begin{bmatrix}{}_i\bar{J}_{nm}\\ {}_i\bar{K}_{nm}\end{bmatrix}=\frac{P_{n+1}(\lambda_i)-P_{n-1}(\lambda_i)}{(2n+1)^2(1-\lambda_i)}\left(\frac{r_i'}{a}\right)^n\times\left(\frac{M_i}{M}\right)\begin{bmatrix}\bar{R}_{nm}(\mu_i',\theta_i')\\ \bar{S}_{nm}(\mu_i',\theta_i')\end{bmatrix}, \tag{6}$$

cap

$$\begin{bmatrix}{}_i\bar{J}_{nm}\\ {}_i\bar{K}_{nm}\end{bmatrix}=\frac{\int_{i\mu_1}^{i\mu_2}P_{nm}(\mu')\,d\mu}{m(2n+1)({}_i\theta_2-{}_i\theta_1)({}_i\mu_1-{}_i\mu_2)}\left(\frac{r_i'}{a}\right)^n\times\left(\frac{M_i}{M}\right)\begin{bmatrix}\sin(m_i\theta_2)-\sin(m_i\theta_1)\\ \cos(m_i\theta_1)-\cos(m_i\theta_2)\end{bmatrix}. \tag{7}$$

rectangle

2.2 Extension of results for elements of volume

Integration of the potential of a surface element over some range of depth yields the potential of a volume element with the same surficial shape. Fig. 2 illustrates a spherical 'cone' and a spherical 'block', the respective volumetric analogues of a spherical cap and rectangle.

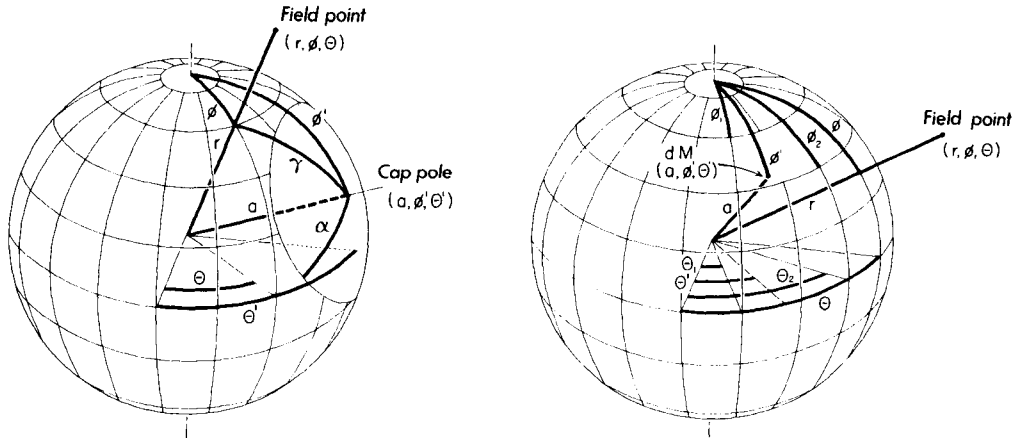

Figure 1. Mass and field coordinates for spherical cap (left) and spherical rectangle (right), situated arbitrarily on reference sphere. Although the elements are illustrated at the surface of the reference sphere, they may be situated at any radius $r' < a$.

Note that the expressions (6) and (7) for the coefficients of surface elements both contain a term which we may define as

$$ {}_i^s\beta_n = (M_i/M)(r_i'/a)^n. \tag{8}$$

The function ${}_i^s\beta_n$ completely describes the mass and radial dependence of the degree n coefficients for the ith surface element; its association with 2-D surface element is denoted by the superscript s.

The mass of a surface element is $M_i = \rho_i \Omega_i (r_i')^2$. The relationship of surface density to volume density $\sigma_i = \rho_i\, dr'$ yields

$$M_i = \rho_i \Omega_i (r_i')^2\, dr'$$

as the mass of the ith surface element. We may then rewrite (8) as

$${}_i^s\beta_n = (\rho_i \Omega_i / M)(r_i')^{n+2}/a^n\, dr'.$$

The potential coefficients ${}_i\bar{J}_{nm}$ and ${}_i\bar{K}_{nm}$ are composed of orthogonal functions of radius, colatitude, and longitude. Because all of the radial position dependence of the coefficients for a surface element (spherical cap or rectangle) is contained in ${}_i^s\beta_n$, integration of ${}_i^s\beta_n$ over a range of the radial coordinate r' yields a term ${}_i^v\beta_n$, which accordingly describes the radial and mass dependence of the coefficients of a mass element distributed through a volume, as denoted by the superscript v:

$${}_i^v\beta_n = \int_{\text{radius}} {}_i^s\beta_n = \int_{ir_1}^{ir_2} \frac{\rho_i \Omega_i}{M_i} \frac{(r_i')^{n+2}}{(a)^n}\, dr'.$$

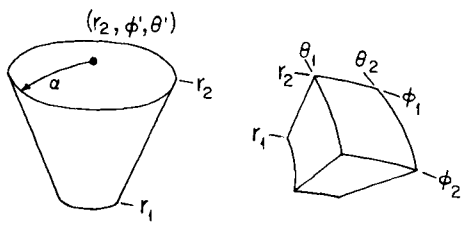

Figure 2. Spherical cone (left) and spherical block (right), obtained by the respective extension of spherical cap and spherical rectangle through the range of radius $r_1 < r' < r_2$.

The inner and outer radii of the volume element are r_1 and r_2, respectively. Carrying out the integration, extracting the term for the element's volume, $v_i = (1/3)\Omega_i(r_2^3 - r_1^3)$, and noting that $M_i = \rho_i v_i$, yields

$${}_i^v\beta_n = \left(\frac{M_i}{M}\right)\left(\frac{{}_ir_2'}{a}\right)^n \left(\frac{3}{n+3}\right)\left[\frac{1-({}_ir_1/{}_ir_2)^{n+3}}{1-({}_ir_1/{}_ir_2)^3}\right]. \tag{9}$$

Because $(M_i/M)(r_2/a)^n$ in (9) is just ${}_i^s\beta_n$ with $r' = r_2$, we obtain

$$\begin{pmatrix} {}_i^v\bar{J}_{nm} \\ {}_i^v\bar{K}_{nm} \end{pmatrix} = \left(\frac{3}{n+3}\right)\left[\frac{1-({}_ir_1/{}_ir_2)^{n+3}}{1-({}_ir_1/{}_ir_2)^3}\right]\begin{pmatrix} {}_i^s\bar{J}_{nm} \\ {}_i^s\bar{K}_{nm} \end{pmatrix} \tag{10}$$

with ${}_i^s\bar{J}_{nm}$ and ${}_i^s\bar{K}_{nm}$ the potential coefficients of a surface mass element at radius r_2, and ${}_i^v\bar{J}_{nm}$ and ${}_i^v\bar{K}_{nm}$ the coefficients of the volume element with the same surficial shape as the surface element but extending between the radii r_1 and r_2. This important result shows that the potential coefficients of a volume element are related to the potential coefficients of the corresponding surface element by a simple function of the radial range which it occupies. In general, we denote the coefficients of the potential of any mass element by ${}_i\bar{J}_{nm}$ and ${}_i\bar{K}_{nm}$. The use of the superscripts s and v, denoting the potential coefficients for elements of surface and volume, respectively, is a temporary expedient designed to increase the clarity of this section; the use of these superscripts will be dropped in the remainder of this paper.

Expression (10) allows the simple computation of the spherical harmonic coefficients of the volume element with the same surficial shape as some surface element. Hence the application of (10) to the potential coefficients of a spherical cap (6) yields the potential coefficients of a spherical cone extending between radii r_1 and r_2. Similarly, we may convert the potential coefficients of a spherical rectangle (7) to the potential coefficients of a spherical block of the same surficial shape.

Figure 3 shows a few of the ways in which spherical volume elements lend themselves to use in modelling tectonic and convectional features within the Earth. A spherical cone can represent a plume, and an appropriately shaped block can model a sheet-like vertical limb of a convection cell. Individual elements may be grouped in

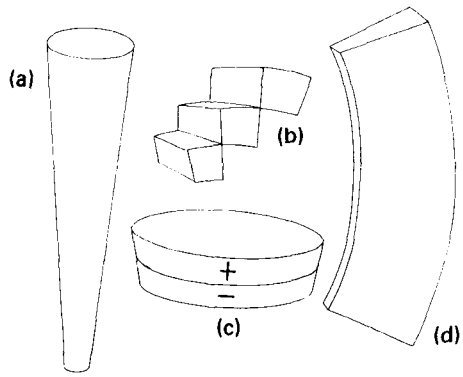

Figure 3. Volume elements defined by spherical coordinates as models for tectonic features. (a) Spherical cone representing a mantle plume beneath a hotspot; (b) several elongate spherical blocks assembled to model a subducted slab; (c) elements with masses of opposite sign stacked vertically to model compensation; (d) long thin spherical block representing a sheet-like zone of vertical upwelling associated with mid-ocean spreading ridges.

ensembles to model more complex features, such as a subducted slab or a compensated body, as shown in Fig. 3.

2.3 Point dipole

The potential of a point dipole may provide a useful approximation for the field of a compensated mass anomaly. An anomalous mass M_i^+ at radius r_i', compensated by an anomalous mass M_i^- lying a distance h directly below, such that $M_i^- = -M_i^+$, may be approximated by a point dipole with a radial dipole moment

$$ {}_iM_r = (M_i^+)(h). \tag{11}$$

The vertically oriented dipole with moment ${}_iM_r$ is the most relevant geophysically. As Dahlen (1982) points out, several definitions of isostasy are possible, each implying a somewhat different distribution of anomalous mass and corresponding differences in the potential fields generated. However, the point dipole should provide a reasonable first-order approximation to an isostatically compensated body.

Hurwitz (1960) gives the potential of a point magnetic dipole at arbitrary radius r_i' within a sphere of radius a. As modified for a gravitational rather than a magnetic dipole, and in terms of the symbols and normalizations used in this paper, the spherical harmonic coefficients for the disturbing potential of a point dipole at arbitrary depth are given by

$$\begin{pmatrix} {}_i\bar{J}_{nm} \\ {}_i\bar{K}_{nm} \end{pmatrix} = \left(\frac{-n}{2n+1}\right)\left(\frac{r_i'}{a}\right)^n \left(\frac{{}_iM_r}{M_i r_i}\right)\begin{bmatrix} \bar{R}_{nm}(\mu_i', \theta_i') \\ \bar{S}_{nm}(\mu_i', \theta_i') \end{bmatrix}. \tag{12}$$

dipole

The expressions (5) and (12) for the coefficients of the disturbing potential of a point mass and a point dipole are quite similar, differing in only two respects. (i) Expression (12) is scaled by $-n/(2n+1)$, rather than $-1/(2n+1)$ as in (5). Hence a point dipole tends to have greater strength in its high-degree potential coefficients than in its low-degree coefficients, whereas a point monopole has greater strength in the low-degree coefficients. (ii) The coefficients for the disturbing potential of a point mass are weighted by the mass ratio (M_i/M), whereas for a point dipole the coefficients are weighted by the ratio of 'moments' ${}_iM_r/(Mr_i')$. Using the definition (11) for radial dipole moment, we may rewrite the ratio of moments as $(M_i/M)(h/r_i')$. In most geophysical applications concerning mass distribution in the mantle, $h \ll r_i'$ and we see that the disturbing potential of a point dipole has considerably less strength than that of a point of mass ${}_iM_r/h$, particularly in the low-degree harmonics.

3 SPECTRAL REPRESENTATION OF GRAVITATIONAL POTENTIAL

The size, shape, mass, geographic location, and depth of a single mass element determine the values of the individual coefficients ${}_i\bar{J}_{nm}$ and ${}_i\bar{K}_{nm}$ given in (5), (6), (7), (10), or (12). The degree variance

$$ {}_i\sigma_n^2 = \sum ({}_i\bar{J}_{nm}^2 + {}_i\bar{K}_{nm}^2) \tag{13}$$

provides a collective measure of the strength of these coefficients. Similarly, the degree variance σ_n^2 of an ensemble of disturbing elements is given by the sum of the squares of the ensemble coefficients $\bar{J}_{nm}$ and $\bar{K}_{nm}$. The set of values for the degree variance is independent of the geographic location of the mass element in question; for example, changing the location of a given spherical cap would not change the values of the degree variance associated with it. However, any change in that cap's size, mass, or depth would generate a set of degree variances with different values.

Pollack (1973) defines the spectrum

$$\Phi_n = \sigma_n(2n+1)^{1/2} \tag{14}$$

which has the property that a point mass at the surface of the sphere $(r' = a)$ has equal spectral strength at every harmonic degree, i.e., Φ_n = constant for all n, as shown in Fig. 4.

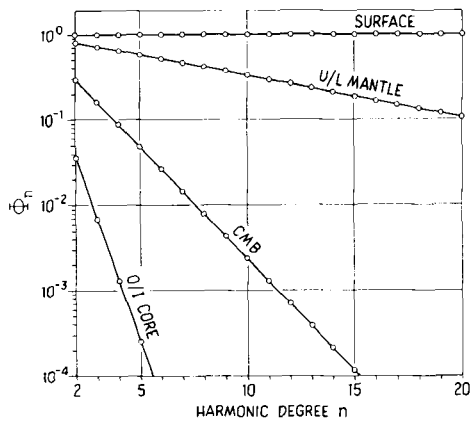

Figure 4. Spectra Φ_n of unit point masses located at various depths: *Surface*: surface of the earth ($r' = 6371$ km); *U/L Mantle*: boundary between upper and lower mantle ($r' = 5701$ km); *CMB*: the core–mantle boundary ($r' = 3486$ km); *O/I Core*: outer–inner core boundary ($r' = 1217$ km). Spectra progressively attenuate with depth of point source; point mass at centre of sphere ($r' = 0$) has spectral strength only at $n = 0$, with strength at all higher degrees identically zero.

The degree one spherical harmonic coefficients $\bar{J}_{1m}$ and $\bar{K}_{1m}$ describe the displacement of the coordinate origin from a body's centre of mass. Because models of the Earth's potential assume the origin at the centre of mass, the $n = 1$ harmonic coefficients of the Earth's potential are zero (Heiskanen & Moritz 1967). Although an isolated mass element does develop some spectral strength at $n = 1$, we display values of the harmonic spectrum in the degree range $2 \leq n \leq 20$. Of course data from surface gravimetry and, over the oceans, geoid heights obtained by satellite altimetry, provide more detail for studying regional and local features, such as the relationship between gravity and topography, as in Watts *et al.* (1985). However, the degree 2 to 20 range is quite appropriate for examination of large-scale patterns of the global field.

Also shown in Fig. 4 are spectra of point masses located below the surface of the sphere; they have less high-degree strength and hence have spectra which are 'reddened' relative to that of a point mass located at the surface. The spectra of masses distributed over a spherical surface, such as a spherical cap or rectangle, also redden when located at greater depths. A cap or rectangle also has less high-degree strength than the same mass concentrated in a point at the same depth. This reddening occurs because the centre of mass of any portion of a spherical shell lies below the radius of the shell. As the size of a cap increases, the centre of mass moves downward, and in the limit of a complete spherical shell, it has the potential of a point mass at its centre, $V = GM/r$, with non-zero spectral strength only in the $n = 0$ term of the potential. Hence all distributions of mass over some area or volume on or within a sphere may be understood simply as cases intermediate between the concentration of that mass in a point at either the surface of a sphere or at its centre. The spectrum generated by any distributed mass element will be intermediate between the flat 'white' spectrum of a point mass at the surface and the zero-valued (for all degrees except $n = 0$) 'red' spectrum of a point mass at the sphere's centre. Fig. 5 illustrates some of these reddening effects.

Figure 6 illustrates the extent to which a point dipole approximates a compensated distribution of mass. Curve (a) is the spectrum of an ensemble consisting of two point masses, one of positive mass located at the Earth's surface and the other of negative mass, located at 40 km depth beneath the first mass. A point dipole having the same dipole moment and located halfway between the two point masses generates a spectrum which, at the scale of the illustration, is identical to that produced by the pair of point masses. Hence, at least through degree 20, the point dipole can provide a convenient and accurate model of crustal scale compensation.

Curve (b) of Fig. 6 is the spectrum generated by two point masses of opposite sign, one at the surface and the other at the base of the mantle transition zone at 670 km depth; for comparison, curve (c) is the spectrum of a point dipole located mid-way between. Both spectra (b) and (c) are generated by distributions having the same dipole moment as that which produced spectrum (a). The two opposite point masses generate a spectrum which is quite similar in degrees 2–10 and differs only slightly in higher degrees from the spectrum of the point dipole. Hence a point dipole provides a satisfactory approximation in the lower degrees of the spectrum of mass distributions which are compensated across the thickness of the upper mantle. Note also that the spectra (b) and (c) are attenuated by depth at all degrees. Curves (d) and (e) in Fig. 6 are the spectra generated by identical point dipoles located at still greater depths. As is the case for the spectra of the other elements considered, the spectrum of a point dipole becomes

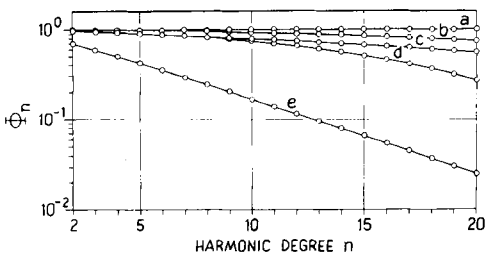

Figure 5. Effect of geometry and depth of distributed unit masses on spectra. The spectra are generated by the following mass elements: (a) point mass at surface of Earth; (b) small spherical cap at surface of earth with generating angle $\alpha = 4°$; (c) volume element with same surficial expression as small cap in (b) but extending from the surface to a depth of 200 km; (d) larger cap with generating angle $\alpha = 8°$ at surface; (e) same small cap as in (b), but located at 1000 km depth. Spectra progressively redden with both increasing depth and extent of mass elements; differences due only to extent of the elements are best discernible in the degree range $n \geq 10$.

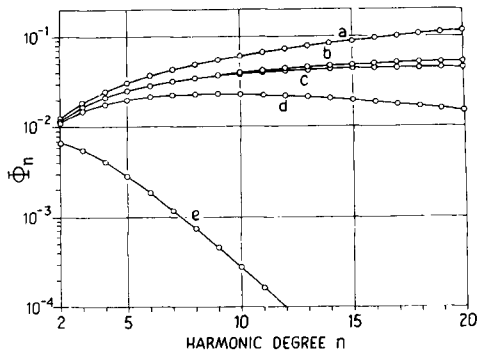

Figure 6. Spectra Φ_n of point dipoles and their approximation by monopoles of opposite sign and finite separation; all generate equal dipole moment. (a) Spectrum generated by an ensemble consisting of two point masses of opposite sign, one at the surface of the Earth and the other directly below it at a depth of 40 km; in the degree range shown, the spectrum of a point dipole of equal dipole moment and located at a depth intermediate between the two point masses is essentially identical. (b) Spectrum generated by two point masses of opposite sign, one at the surface of the Earth and the other 670 km beneath it. (c) Spectrum of a point dipole of dipole moment equal to distribution in (b), and located at depth mid-way between the two point masses. Further depth-dependent attenuation of dipole spectra Φ_n is illustrated by curves (d) and (e); each represents spectrum of a point dipole having the same moment as in (a), (b), and (c) above, but situated respectively at depths of 670 km (base of mantle transiton zone) and 2885 km (core–mantle boundary).

increasingly attenuated, especially in the high degrees, as the dipole is located deeper in the earth.

5 CONCLUSIONS

We have generalized for arbitrary source depth the expressions of Pollack (1973) for the gravitational potential due to a point mass, a spherical cap, and a spherical rectangle, and have developed similar expressions for the potentials of elements of volume defined in the spherical coordinate system. We also have modified Hurwitz's (1960) result for the potential of a magnetic point dipole, to enable computation of the coefficients for the gravitational potential generated by a gravitational dipole representing compensated mass distributions. The spectrum Φ_n provides a useful summary of the properties of the gravitational potential generated by either an isolated mass element or by an ensemble of elements.

The spectrum Φ_n of a point mass at the surface of the Earth has equal strength in all harmonic degrees; at the opposite extreme, the spectrum of a point mass located at the centre of the Earth has spectral strength only in the degree 0 term. These two spectra serve as a convenient and instructive pair of references to which other spectra may be compared. In general, mass elements which are of limited areal or radial extent, or are located close to the surface of the Earth, generate relatively flat spectra, similar to that of a point mass located at the surface of the Earth. Conversely, mass elements which are of large areal or radial extent, or which are located at substantial depth, generate relatively steep, reddened spectra, i.e., spectra which are progressively attenuated in the higher degrees. Compensated bodies, whether represented by a point dipole or by an ensemble of positive and negative mass elements, generate spectra with depressed low-degree strength, and high-degree strength which rises toward that which would be generated by an uncompensated body of mass M_r/h and located at the outer radius of the compensated body.

In the following paper (Jackson *et al.*, paper II) we make use of the analytical results presented here to model the observed spectrum of the Earth's gravitational field, and infer some general characteristics of the distribution of heterogeneity within the Earth.

ACKNOWLEDGMENTS

Stephen Sutton was supported by a National Science Foundation Graduate Fellowship.

REFERENCES

Bowin, C., Simon, B. & Wollenhaupt, W. R., 1975. Mascons: a two-body solution, *J. geophys. Res.*, **80,** 4947–4955.

Chase, C. G., 1979. Subduction, the geoid, and lower mantle convection, *Nature*, **282,** 464–468.

Chase, C. G. & McNutt, M. K., 1982. The geoid: effect of compensated topography and uncompensated oceanic trenches, *Geophys. Res. Lett.*, **9,** 29–32.

Crough, S. T. & Jurdy, D. M., 1980. Subducted lithosphere, hotspots, and the geoid, *Earth planet. Sci. Lett.*, **48,** 15–22.

Dehlen, F. A., 1982. Isostatic geoid anomalies on a sphere, *J. geophys. Res.*, **87,** 3943–3947.

Heiskanen, W. A. & Moritz, H., 1967. *Physical Geodesy*, pp. 29–31, 61–62, Freeman, San Francisco.

Hellinger, S. J., 1983. A method for computing the geoid height contribution of three-dimensional bodies within a spherical earth, *Geophysics*, **48,** 1664–1670.

Hurwitz, L., 1960. Eccentric dipoles and spherical harmonic analysis, *J. geophys. Res.*, **65,** 2555–2556.

Jackson, M. J., Pollack, H. N. & Sutton, S. T., 1991. On the distribution of anomalous mass within the Earth: forward models of the gravitational potential spectrum using ensembles of discrete mass elements, *Geophys. J. Int.*, **107,** 83–94.

Johnson, L. R. & Litehiser, J. J., 1972. A method for computing the gravitational attraction of three-dimensional bodies in a spherical or ellipsoidal earth, *J. geophys. Res.*, **77,** 6999–7009.

Lowrey, B. E., 1978. Lateral density anomalies and the earth's gravitational field, *Rep. No. NASA TM-79554*, NASA-Goddard SFC, Greenbelt, MD.

McAdoo, D. C., 1981. Geoid anomalies in the vicinity of subduction zones, *J. geophys. Res.*, **86,** 6073–6090.

Pollack, H. N., 1973. Spherical harmonic representation of the gravitational potential of a point mass, a spherical cap, and a spherical rectangle, *J. geophys. Res.*, **78,** 1760–1768.

Reasenberg, R. D., Goldberg, Z. M., MacNeil, P. E. & Shapiro, I. I., 1981. Venus gravity: a high resolution map, *J. geophys. Res.*, **86,** 7173–7179.

Sjogren, W. L., Bills, B. G. & Mottinger, N. A., 1984. Venus: Ishtar gravity anomaly, *Geophys. Res. Lett.*, **11,** 489–491.

Takin, M. & Talwani, M., 1966. Rapid computation of the gravitational attraction of topography on a spherical earth, *Geophys. Prosp.*, **14,** 119–142.

Talwani, M., 1973. Computer usage in the computation of gravity anomalies, *Meth. Comp. Phys.*, **13,** 343–389.

Talwani, M. & Ewing, M., 1960. Rapid computation of gravitational attraction of three-dimensional bodies of arbitrary shape, *Geophysics*, **25,** 203–225.

Watts, A. B., McKenzie, D. P., Parsons, B. E. & Roufosse, M., 1985. The relationship between gravity and bathymetry in the Pacific Ocean, *Geophys. J. R. astr. Soc.*, **83,** 263–298.